2-D Membrane Protein Crystallography at Future XFELs

Cameron M. Kewish

Swiss Light Source, Paul Scherrer Institut, CH-5232 Villigen PSI, Switzerland

Email: *cameron.kewish@psi.ch*

Collaborators

Pierre Thibault, Oliver Bunk

Coherent Small Angle X-ray Scattering group (cSAXS)

Swiss Light Source, Paul Scherrer Institut

Franz Pfeiffer

Department Physik (E17)

Technische Universität München, Germany

(Previously at Paul Scherrer Institut & École Polytechnique Fédérale de Lausanne)

Basics of Coherent Diffractive Imaging

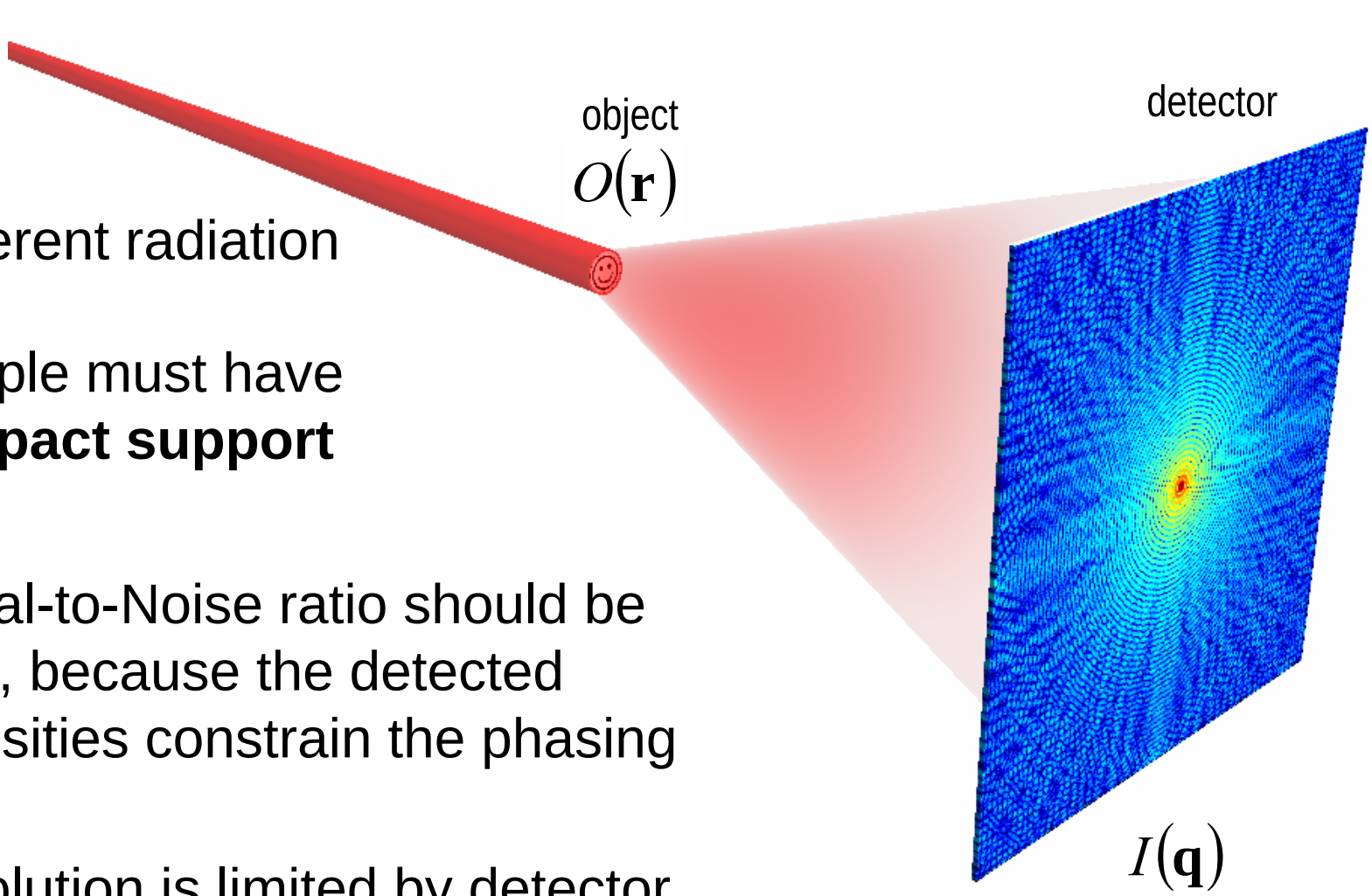

Coherent radiation

Sample must have
compact support

Signal-to-Noise ratio should be
high, because the detected
intensities constrain the phasing

Resolution is limited by detector
solid angle and photon counting statistics…

From parallel to focused beam geometry

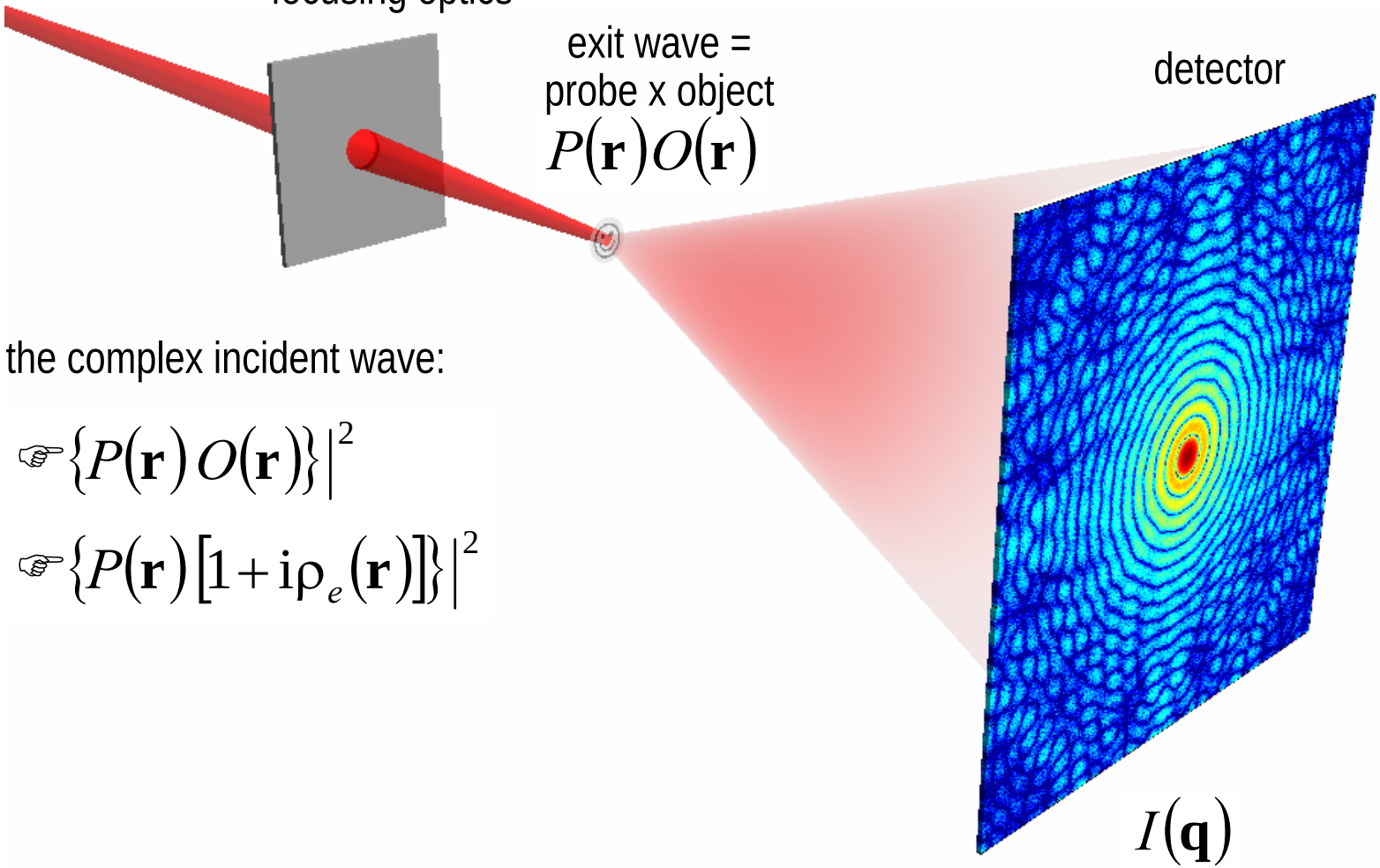

Including the complex incident wave:

$$I(\mathbf{q}) \sim \left| \mathcal{F}\{P(\mathbf{r})\,O(\mathbf{r})\} \right|^2$$

$$\sim \left| \mathcal{F}\{P(\mathbf{r})\,[1 + \mathrm{i}\rho_e(\mathbf{r})]\} \right|^2$$

Real-space support provided by probe

From parallel to focused beam geometry

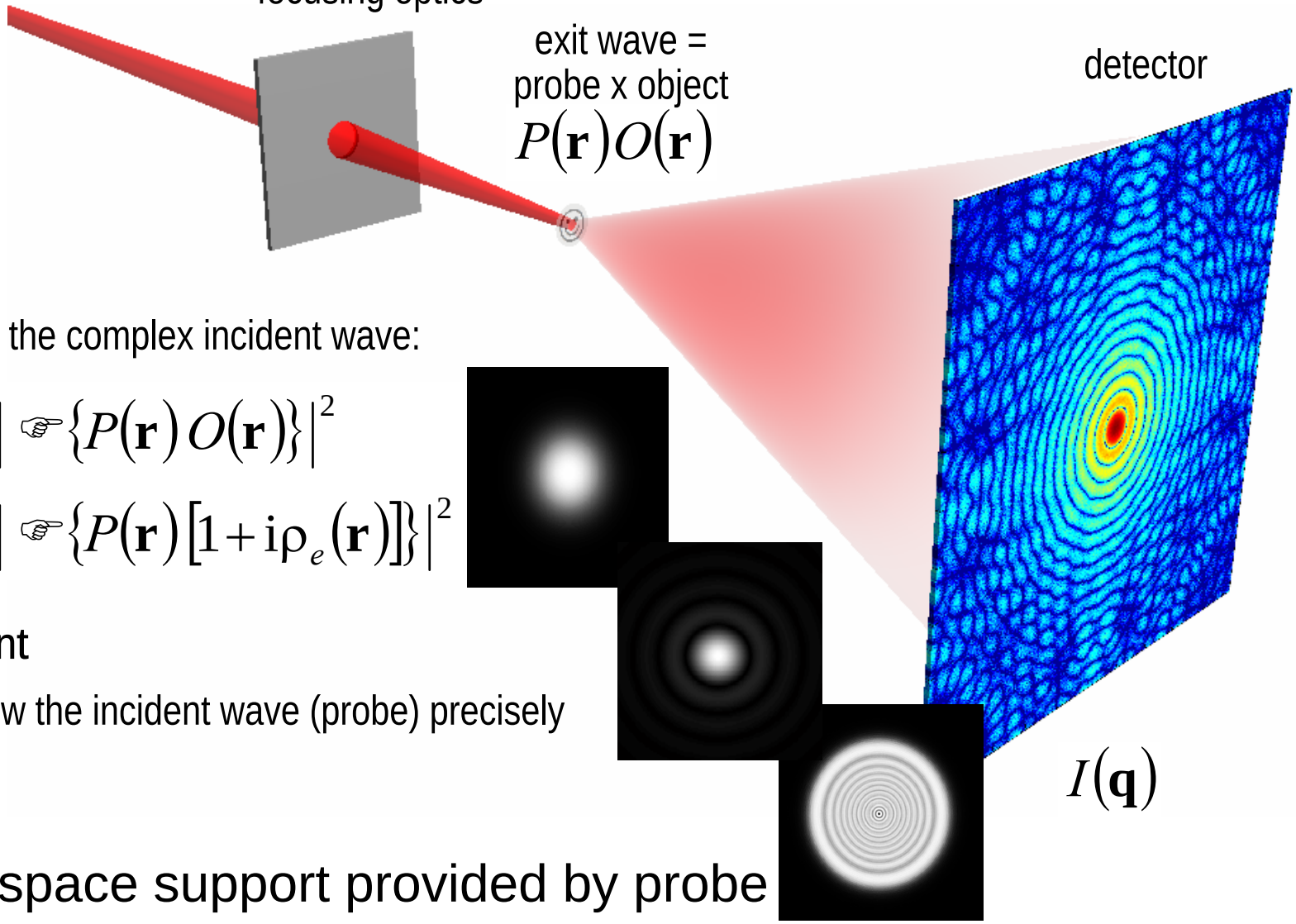

Including the complex incident wave:

$$I(\mathbf{q}) \sim \left| \mathcal{F}\{P(\mathbf{r})\,O(\mathbf{r})\} \right|^2$$

$$\sim \left| \mathcal{F}\{P(\mathbf{r})\,[1+\mathrm{i}\rho_e(\mathbf{r})]\} \right|^2$$

Important

Must know the incident wave (probe) precisely

Real-space support provided by probe

From parallel to focused beam geometry

XFEL pulse

focusing opti

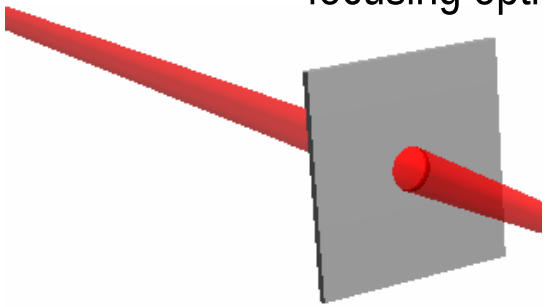

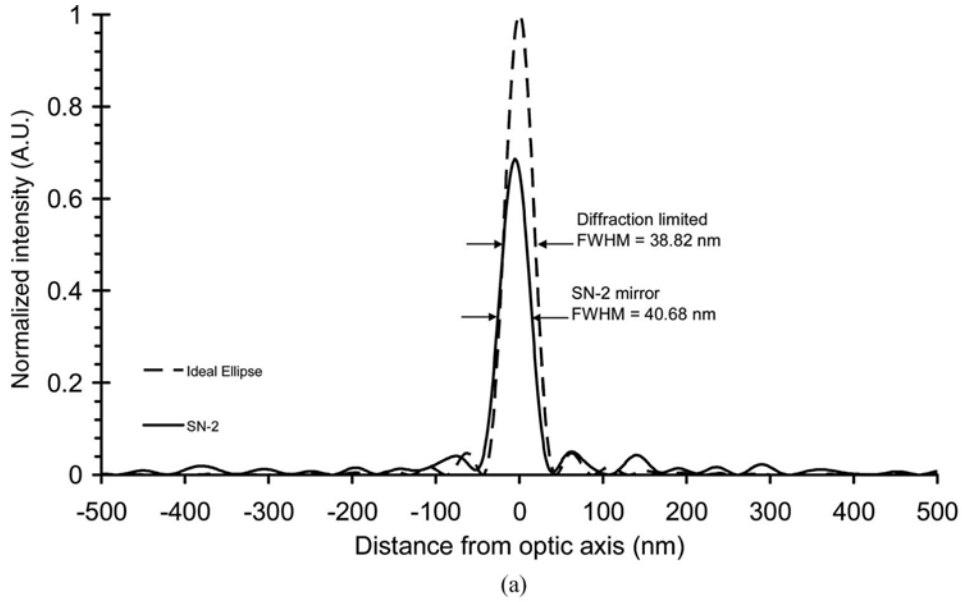

Including the complex incident wave:

$$I(\mathbf{q}) \sim \left| \mathcal{F}\{P(\mathbf{r})\,O(\mathbf{r})\} \right|^2$$

$$\sim \left| \mathcal{F}\{P(\mathbf{r})\,[1+\mathrm{i}\rho_e(\mathbf{r})]\} \right|^2$$

Important

Must know the incident wave precisely

Separate contributions from aberrations of focus and specimen diffraction pattern

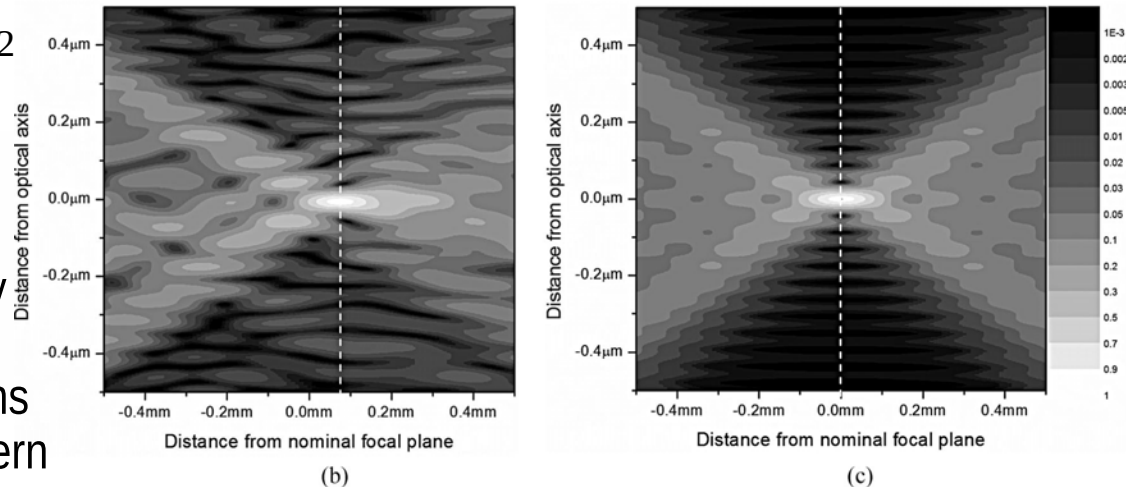

C.M. Kewish et al., *Appl. Opt.* **46**, 2010 (2007)

Ptychographic CDI

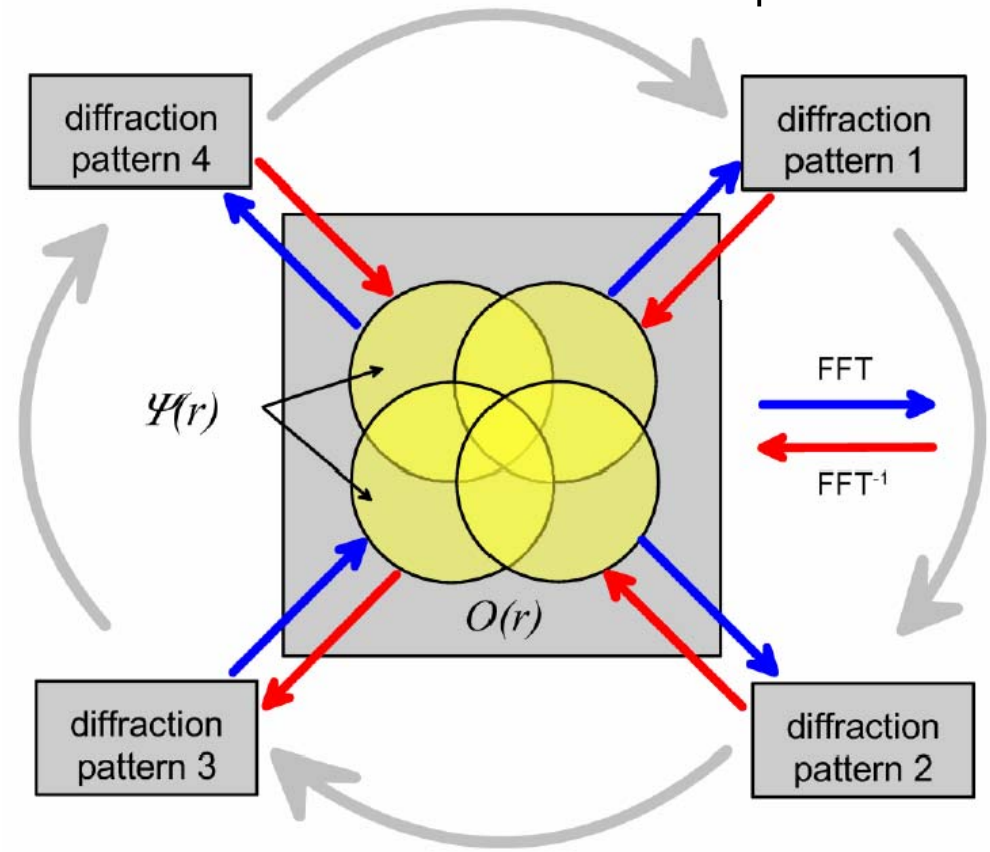

current estimate of object

probe

complex exit wave

$$\psi(\mathbf{r},\mathbf{R}) = O_n(\mathbf{r})P(\mathbf{r}-\mathbf{R})$$

apply Fourier space constraints

$$O_{n+1}(\mathbf{r}) = O_n(\mathbf{r}) + U(\mathbf{r}-\mathbf{R})(\psi_{c,n}(\mathbf{r},\mathbf{R}) - \psi_n(\mathbf{r},\mathbf{R}))$$

update function

$$\frac{|P(\mathbf{r}-\mathbf{R})|}{|P_{\max}(\mathbf{r}-\mathbf{R})|}\frac{P^*(\mathbf{r}-\mathbf{R})}{(|P(\mathbf{r}-\mathbf{R})|^2+\alpha)}$$

move to next aperture position

J.M. Rodenburg & H.M.L. Faulkner, PRL **98**, 034801 (2007)

Ptychography with difference map

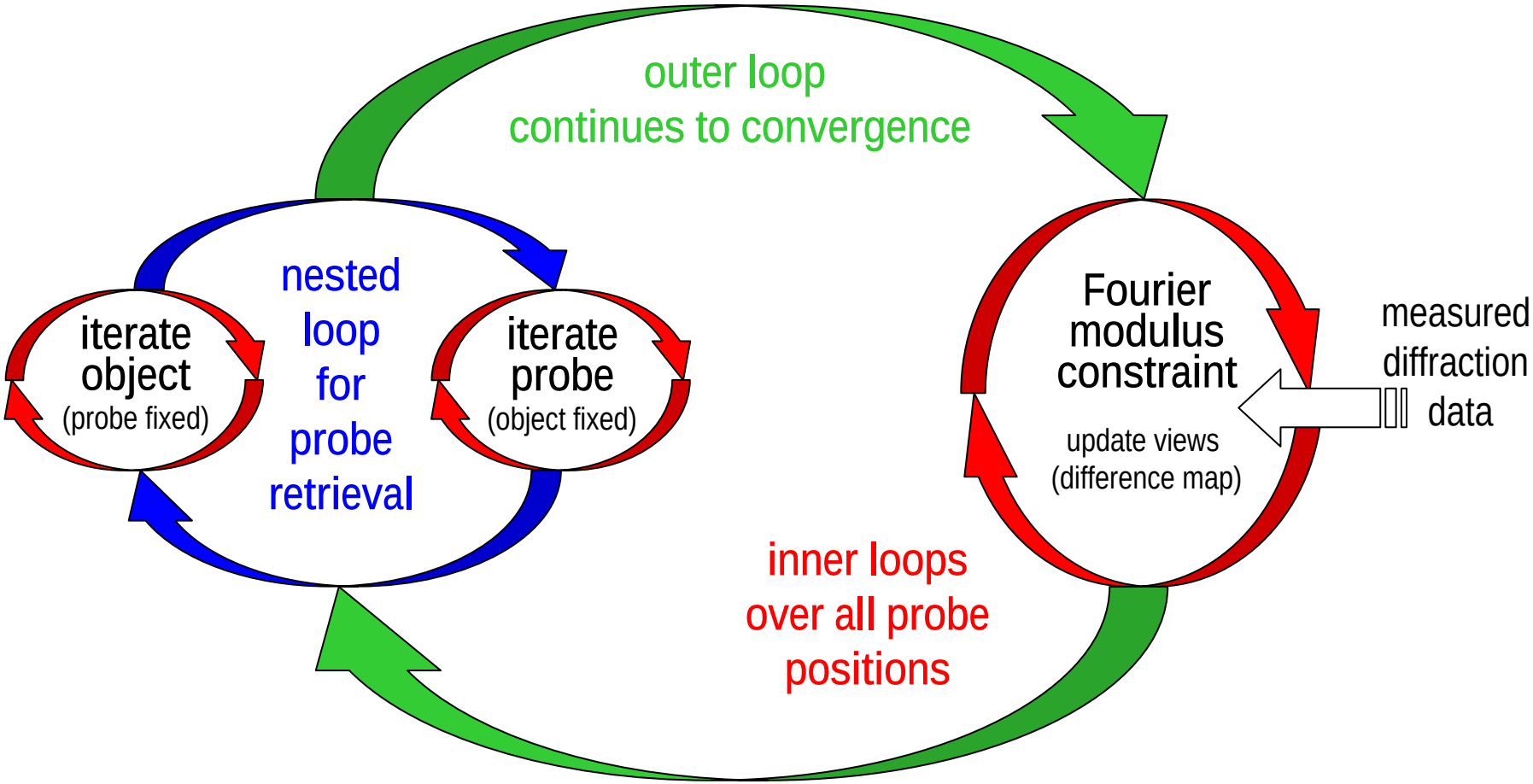

Overlap constraint

Applies known probe positions and uses coupled equations for the probe and object to refine the illumination function

Fourier constraint

Applies measured diffraction amplitudes and keeps the calculated phases

P. Thibault et al. *Ultramicroscopy* **109**, 338 (2009)

“Why?”

1. Why XFEL? Source must be bright enough to get information before damage
2. Why 2D crystals? Many relevant proteins do not form 3D crystals, and are active in 2D crystal form
3. XFEL pulses destroy the sample, but we have many copies of the sample
4. Having multiple copies of the unit cell in the beam improves the signal-to-noise
5. They restrict orientation to in-plane rotation and translation
6. If diffraction patterns can be registered in 2D, we can take ‘mostly’ overlapping exposures – within a unit cell translation in each axis → Ptychography
7. Reconstructing a projection from multiple exposures exploits the redundant info
8. Combining Ptychography and Tomography allows a 3D electron density map to be reconstructed.

Obtaining membrane protein structures…

… with X-rays demands big crystals: microns in size.

Some of the most scientifically relevant proteins are impossible to crystallize

There is no guarantee that the crystal form of the protein is representative of the form in vivo.

Can one determine the structure of a protein without large 3D crystals?

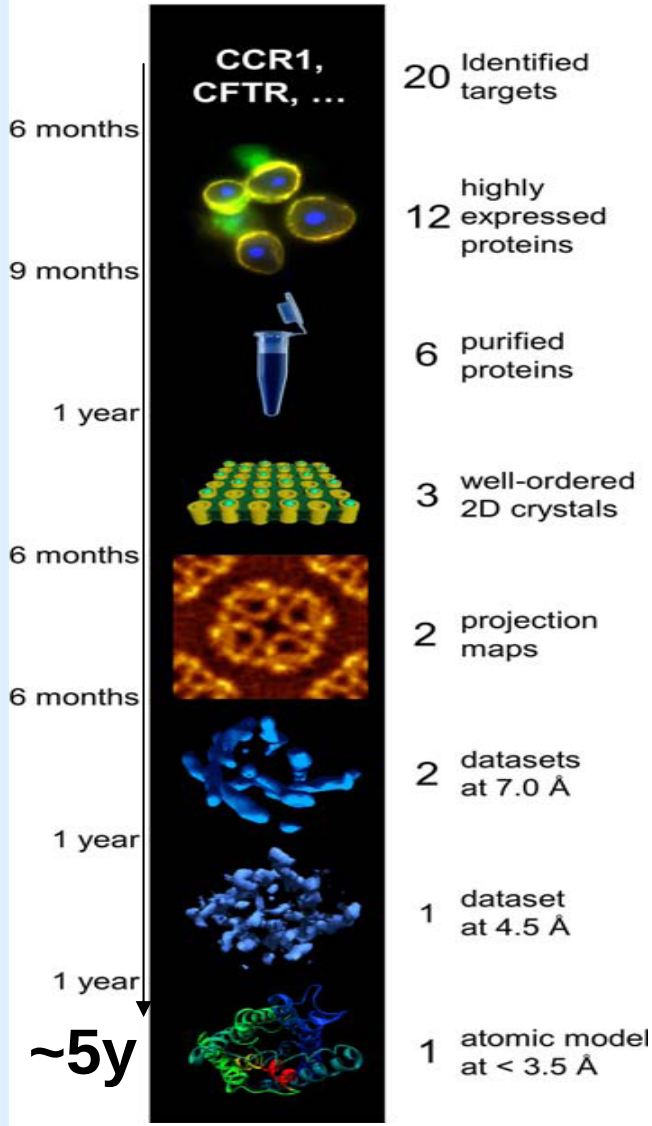

Renault *et al. J Comput Aided Mol Des* **20**, 519 (2006)

2D membrane protein crystals

Engel et al., *Curr. Opin. Struct. Biol.* **18** (2007)

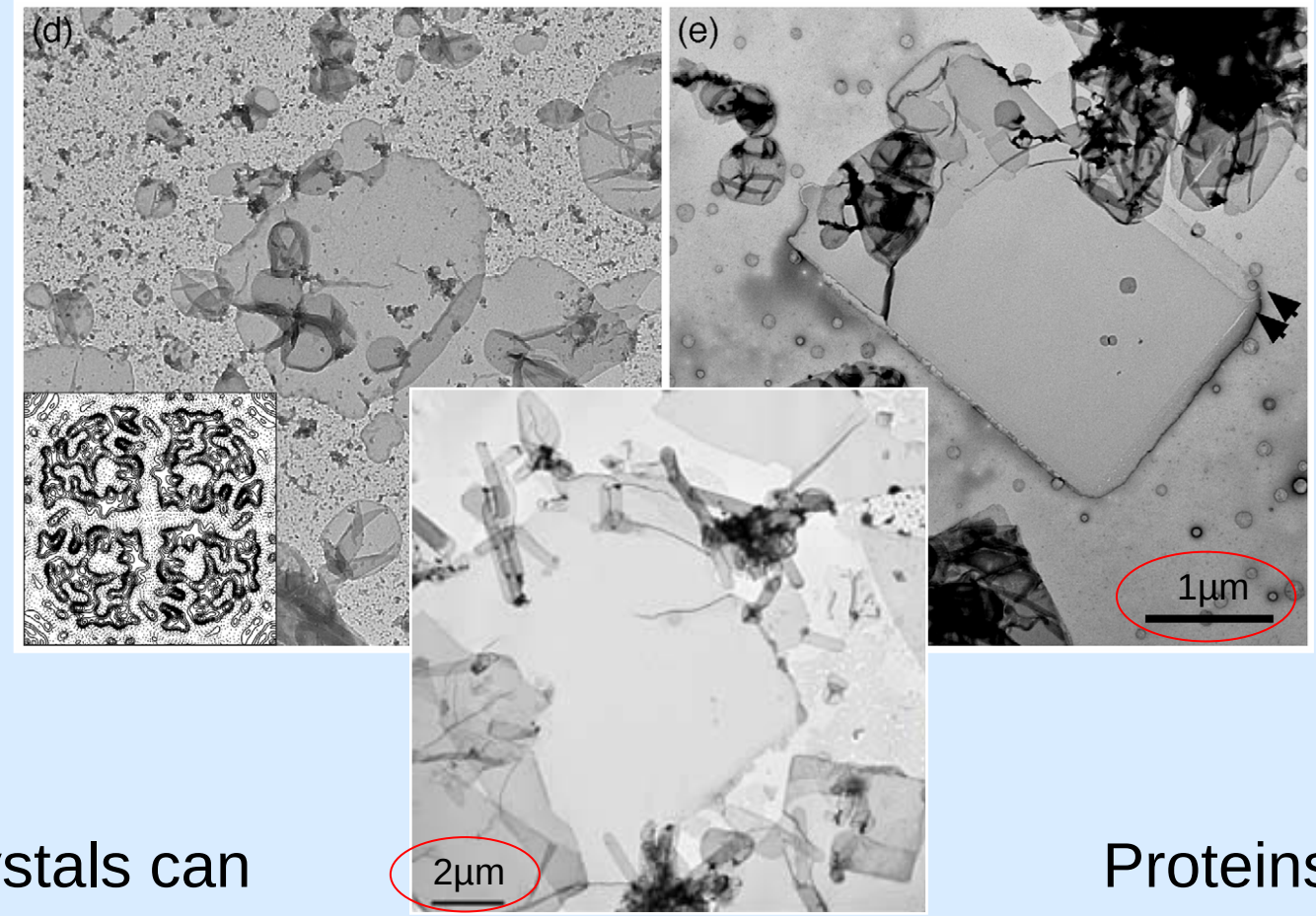

Gonen et al., *Nature* **438** (2005)

2D crystals can be grown

Proteins in native state

Schematic of the simulated experiments

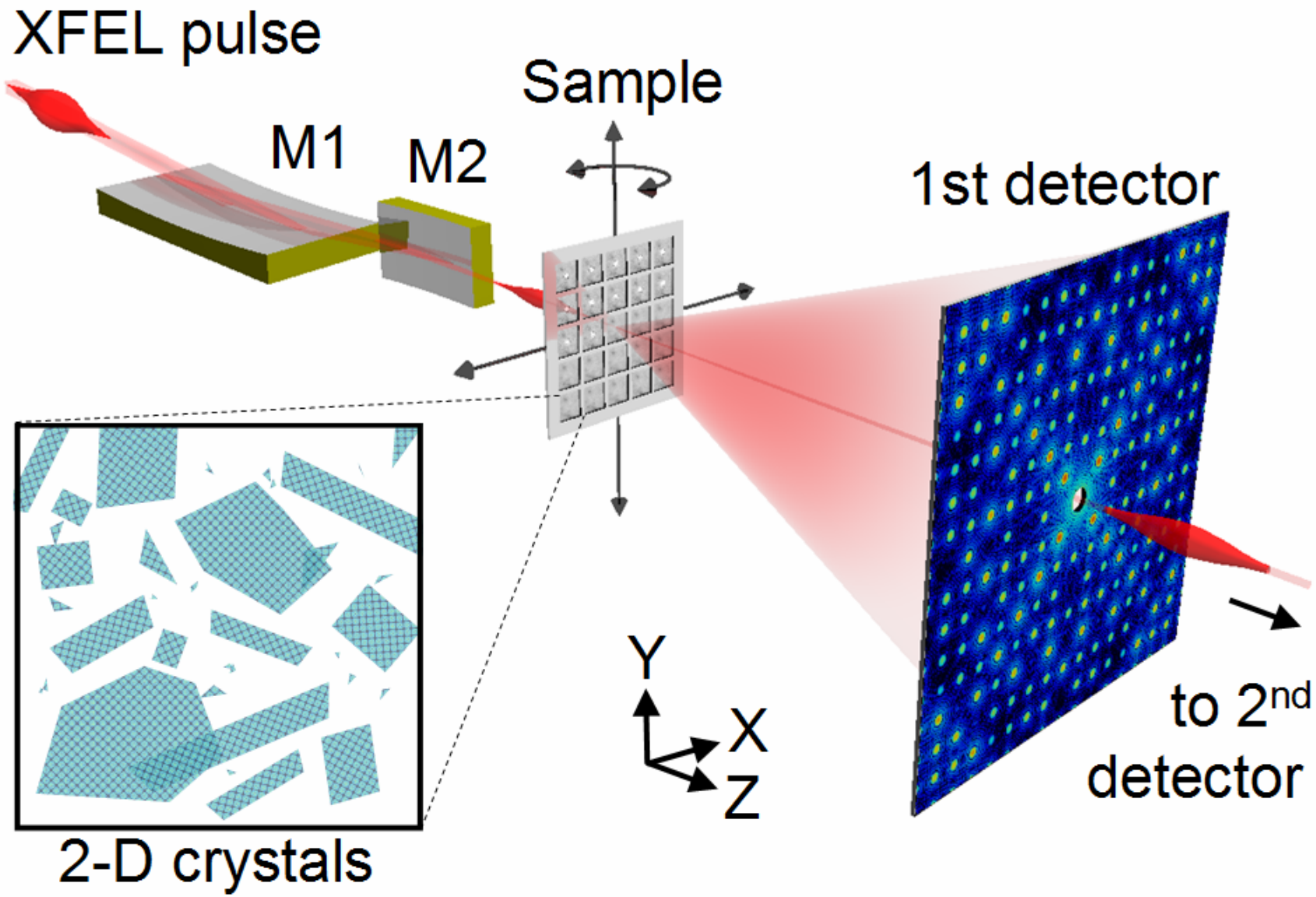

Summary of the simulated experiments

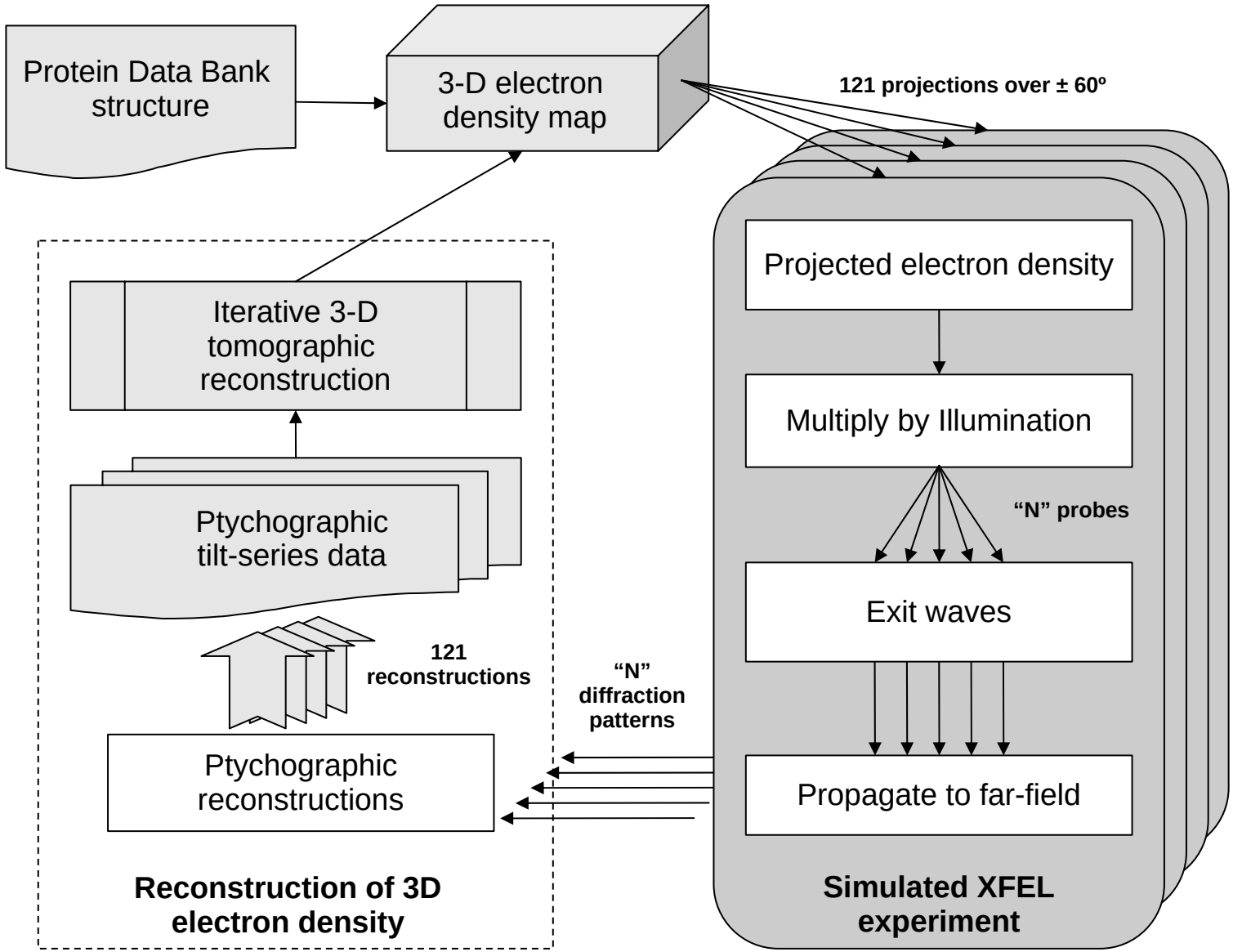

Generating 3D electron density from PDB

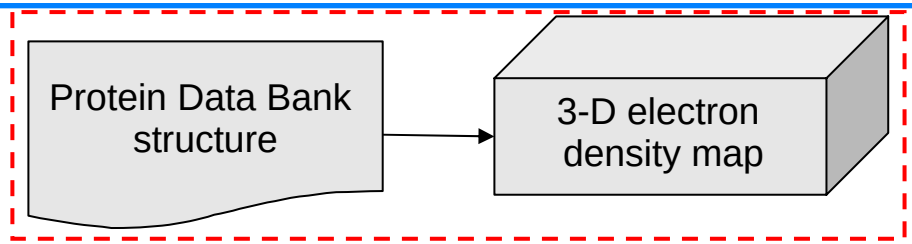

Unit Cell of Aquaporin-1

```
HEADER    MEMBRANE PROTEIN                        07-SEP-00   1FQY
TITLE     STRUCTURE OF AQUAPORIN-1 AT 3.8 A RESOLUTION BY ELECTRON
TITLE    2 CRYSTALLOGRAPHY
AUTHOR    K.MURATA,K.MITSUOKA,T.HIRAI,T.WALZ,P.AGRE,J.B.HEYMANN,
AUTHOR   2 A.ENGEL,Y.FUJIYOSHI
REVDAT   1   18-OCT-00 1FQY    0
JRNL        AUTH   K.MURATA,K.MITSUOKA,T.HIRAI,T.WALZ,P.AGRE,
JRNL        AUTH 2 J.B.HEYMANN,A.ENGEL,Y.FUJIYOSHI
JRNL        TITL   STRUCTURAL DETERMINANTS OF WATER PERMEATION
JRNL        TITL 2 THROUGH AQUAPORIN-1.
JRNL        REF    NATURE                           V. 407   599 2000
JRNL        REFN   ASTM NATUAS  UK ISSN 0028-0836
REMARK   1
REMARK   2
REMARK   2 RESOLUTION. 3.80 ANGSTROMS.
                                .
                                .
ATOM     1  N   LYS A   8 |  56.812  30.226  17.376 | 1.00  10.00 |  N
ATOM     2  CA  LYS A   8 |  57.972  30.061  16.444 | 1.00  10.00 |  C
ATOM     3  C   LYS A   8 |  57.595  28.971  15.486 | 1.00  10.00 |  C
ATOM     4  O   LYS A   8 |  57.990  28.922  14.332 | 1.00  46.93 |  O
ATOM     5  CB  LYS A   8 |  59.210  29.616  17.216 | 1.00  46.93 |  C
ATOM     6  CG  LYS A   8 |  59.575  30.484  18.403 | 1.00  46.93 |  C
ATOM     7  CD  LYS A   8 |  59.667  31.974  17.988 | 1.00  46.93 |  C
ATOM     8  CE  LYS A   8 |  59.865  32.934  19.166 | 1.00  46.93 |  C
ATOM     9  NZ  LYS A   8 |  59.935  34.336  18.667 | 1.00  46.93 |  N
ATOM    10  N   LEU A   9 |  56.864  28.048  16.039 | 1.00  10.00 |  N
                                .
                                .
                                .
```

~1,660 atoms in monomer
MW ~ 28 kDa

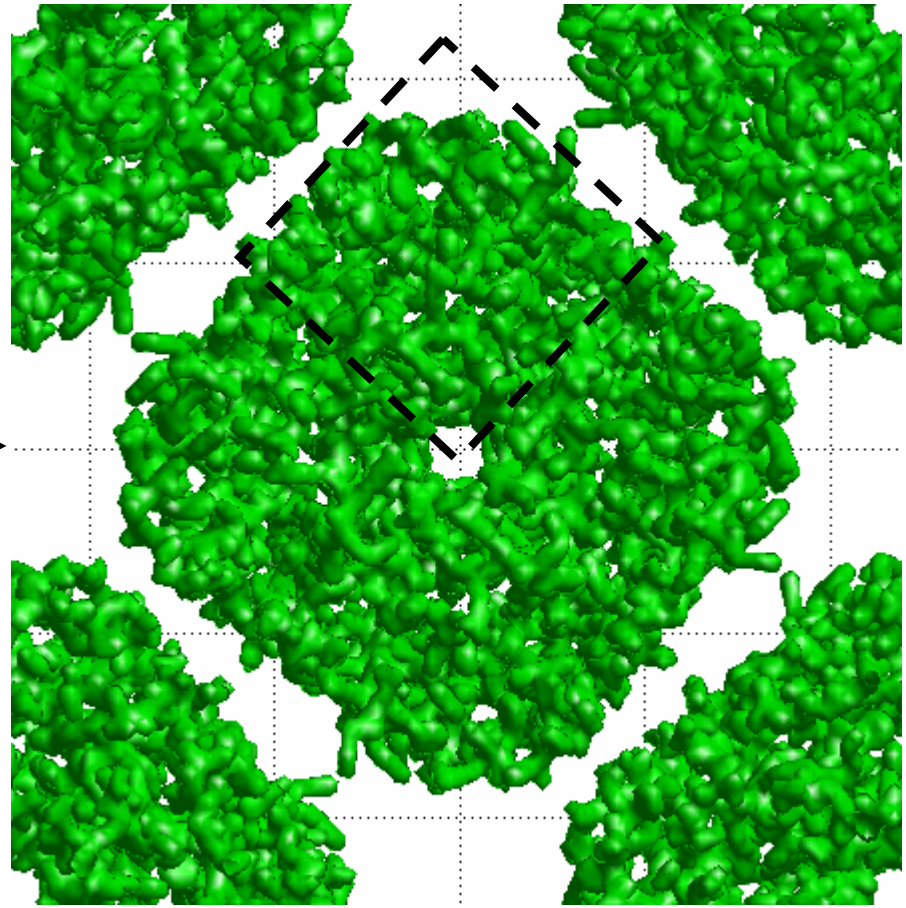

~13,300 atoms in unit cell

Electron density projected into 2D

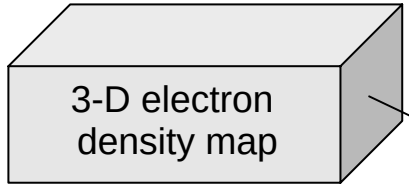

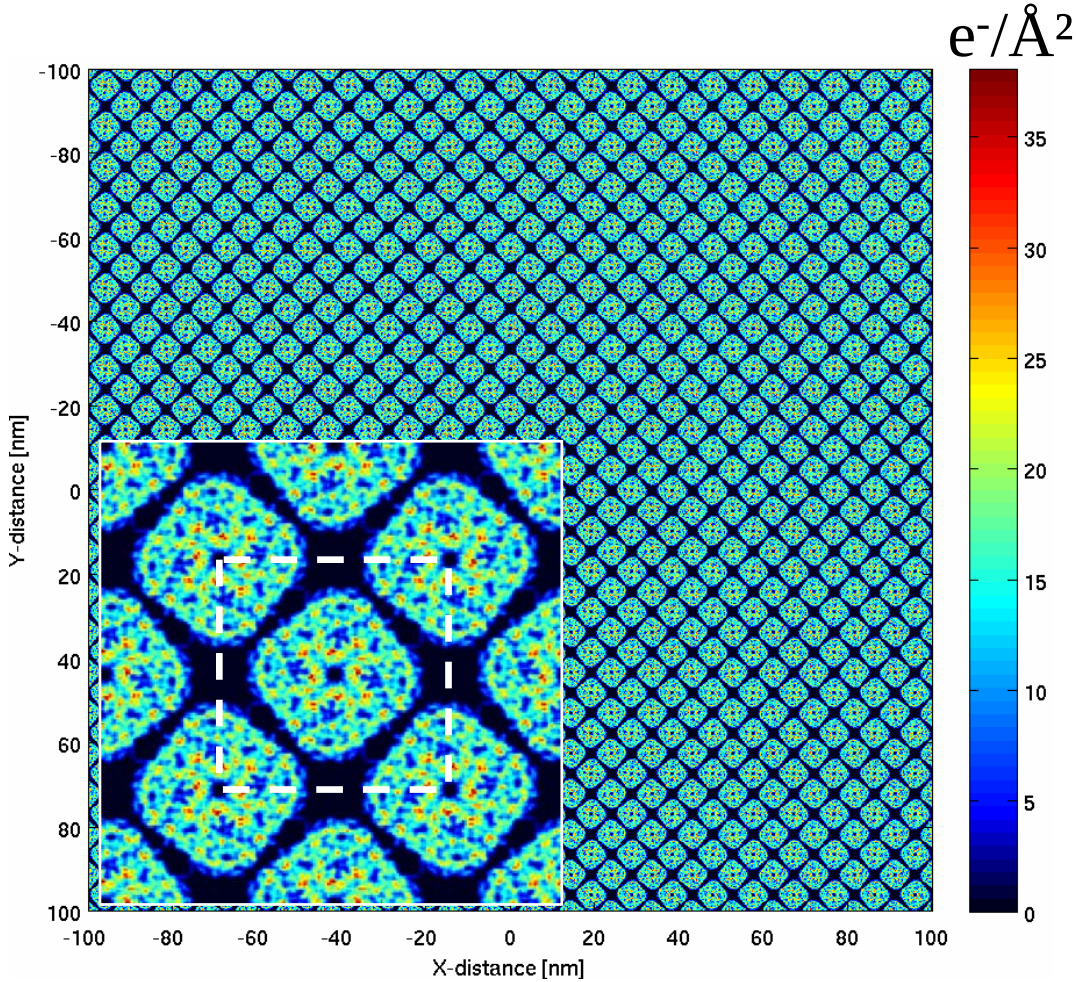

Projected electron density

$$\rho_\theta(x,y) = \int \mathbf{R}(\theta)\rho(x,y,z)\,\mathrm{d}z$$

Complex object
transmission function

$$T(x,y) \approx \exp\left[-\mathrm{i}\, r_e \lambda \rho_\theta(x,y)\right]$$

Simulated XFEL experiment

Simulated XFEL Experiment

Weak phase object ~ 10^{-4}-10^{-3} radians

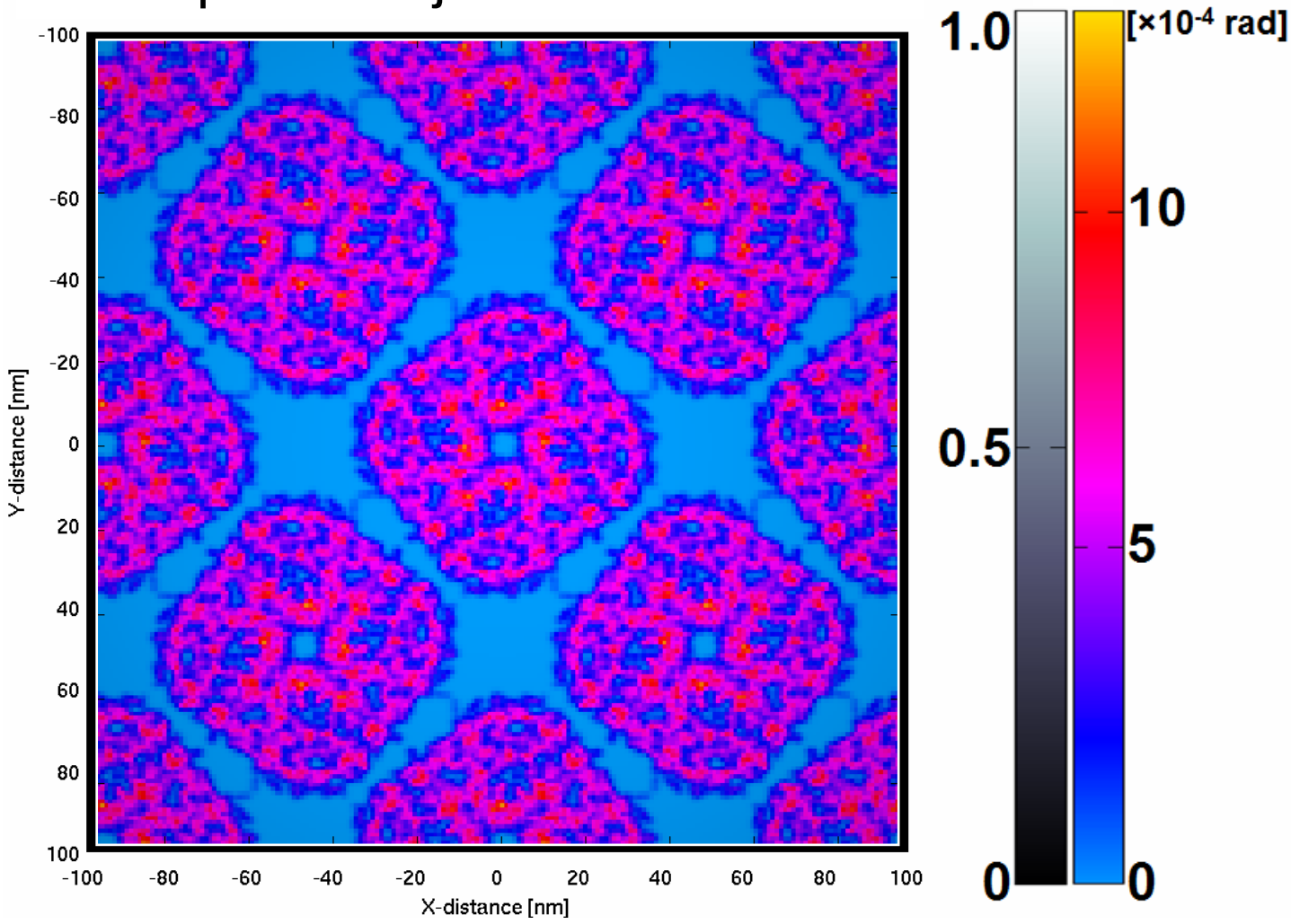

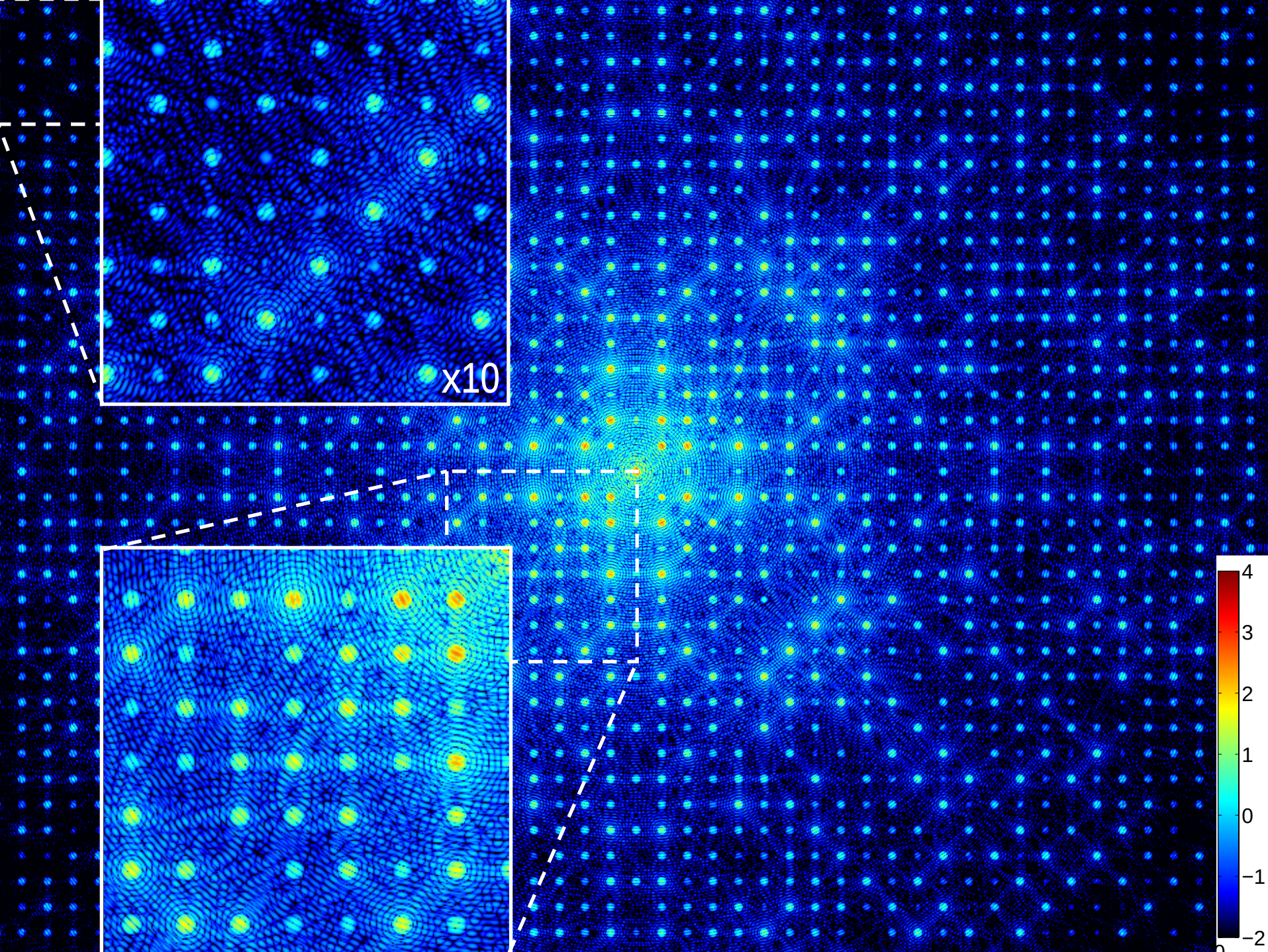
x10
4
3
2
1
0
−1
−2

How does the coherence help?

Interference between diffraction from the aperture and the crystal in between the Bragg peaks changes with the position of the illuminating probe.

Using multiple *"overlapping"* exposure positions, the interference structure allows us to solve the phase problem with a ptychography algorithm.

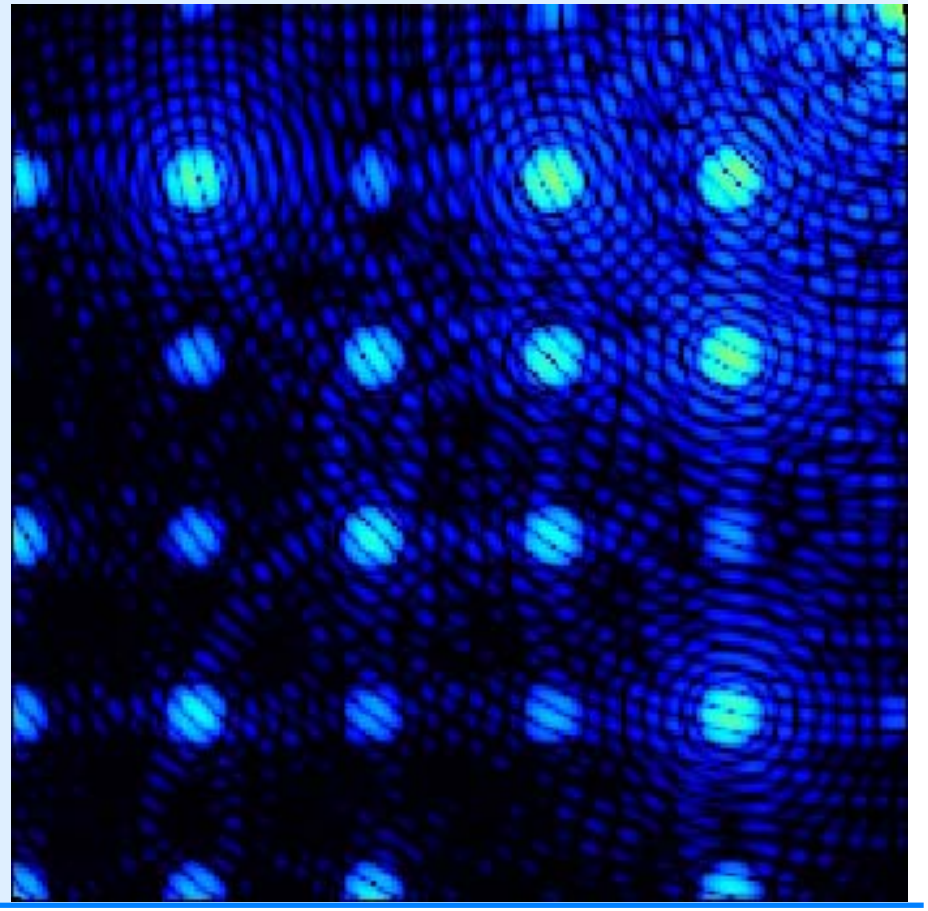

Simulated XFEL experiment

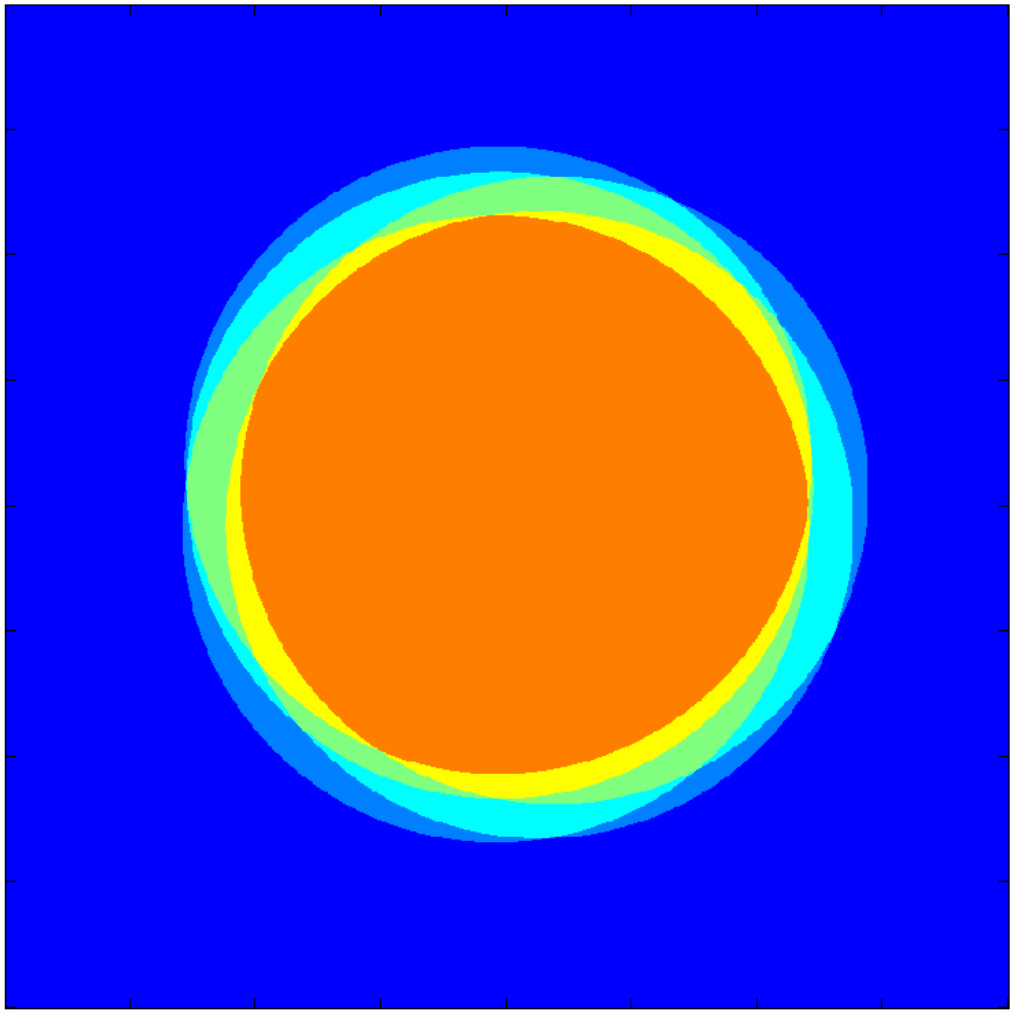

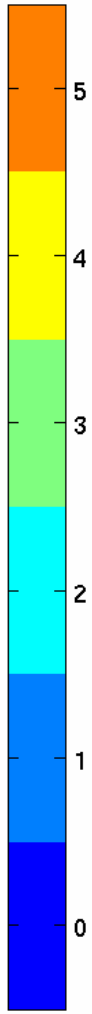

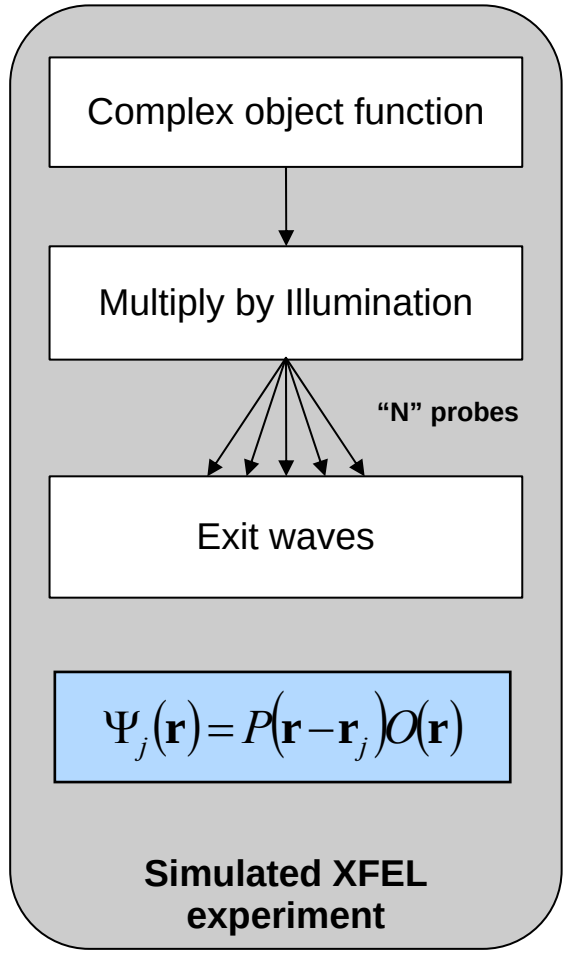

Reconstruction from coherent diffraction

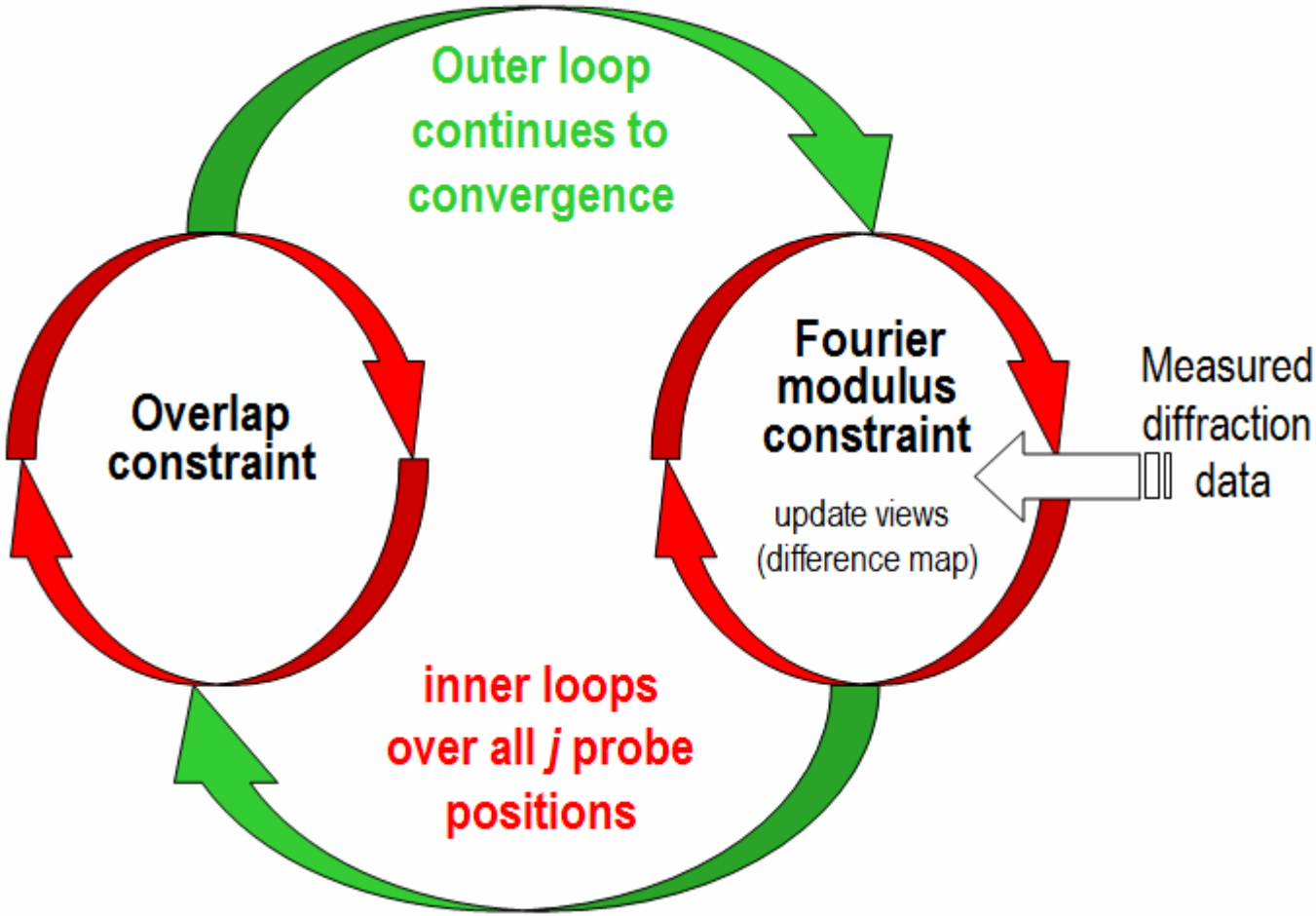

Reconstruction from coherent diffraction

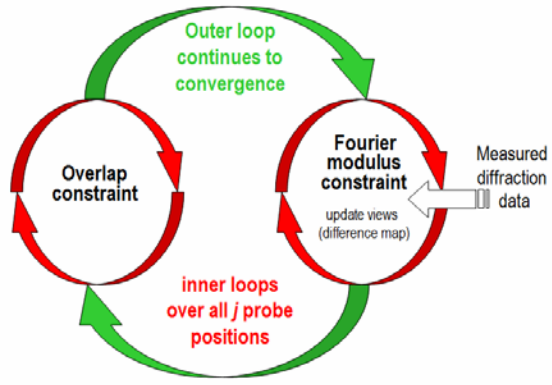

Ptychographic reconstructions

Reconstruction of 3D electron density

Reconstructed exit wave phase

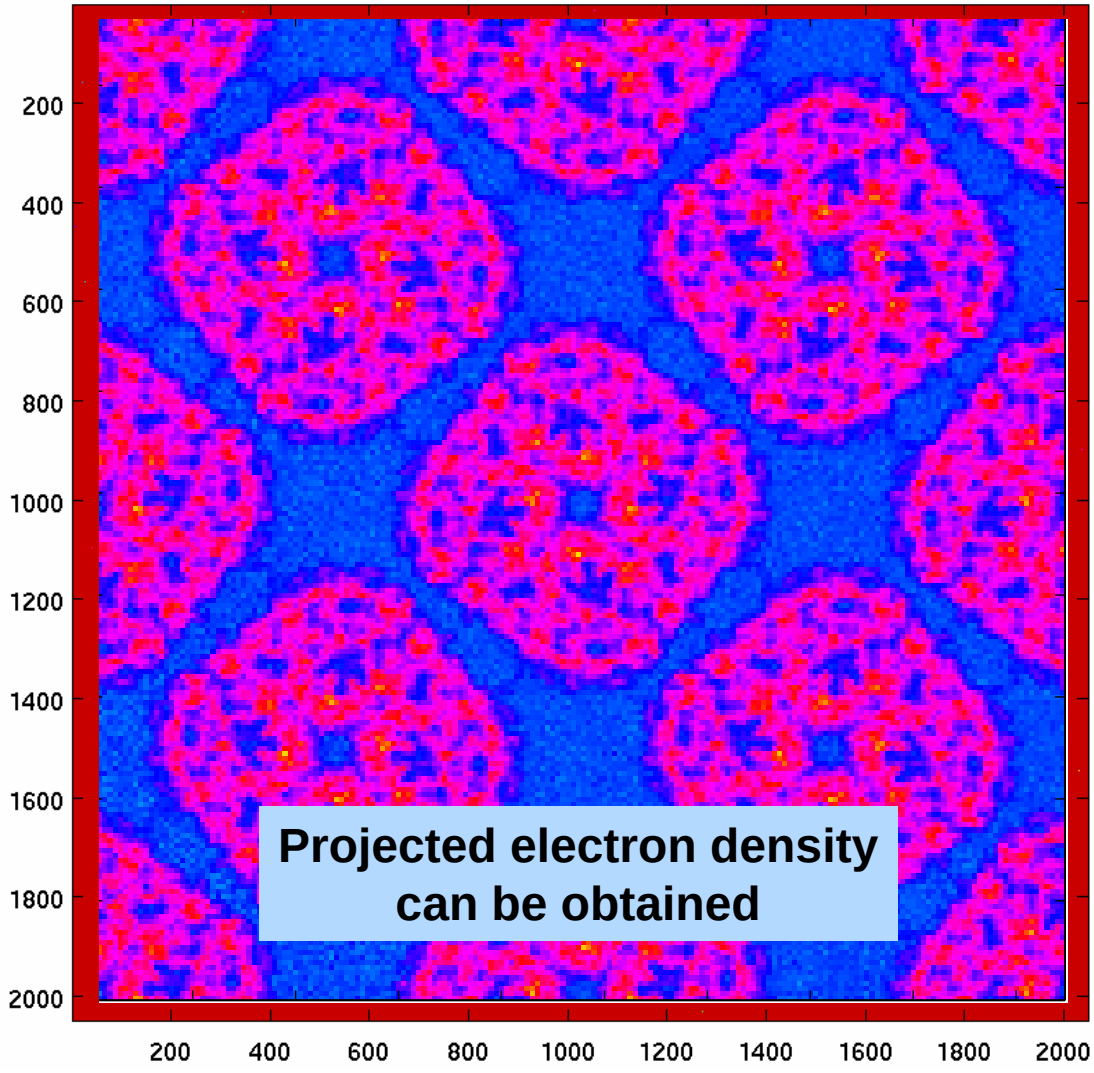

Summary of the simulated experiments

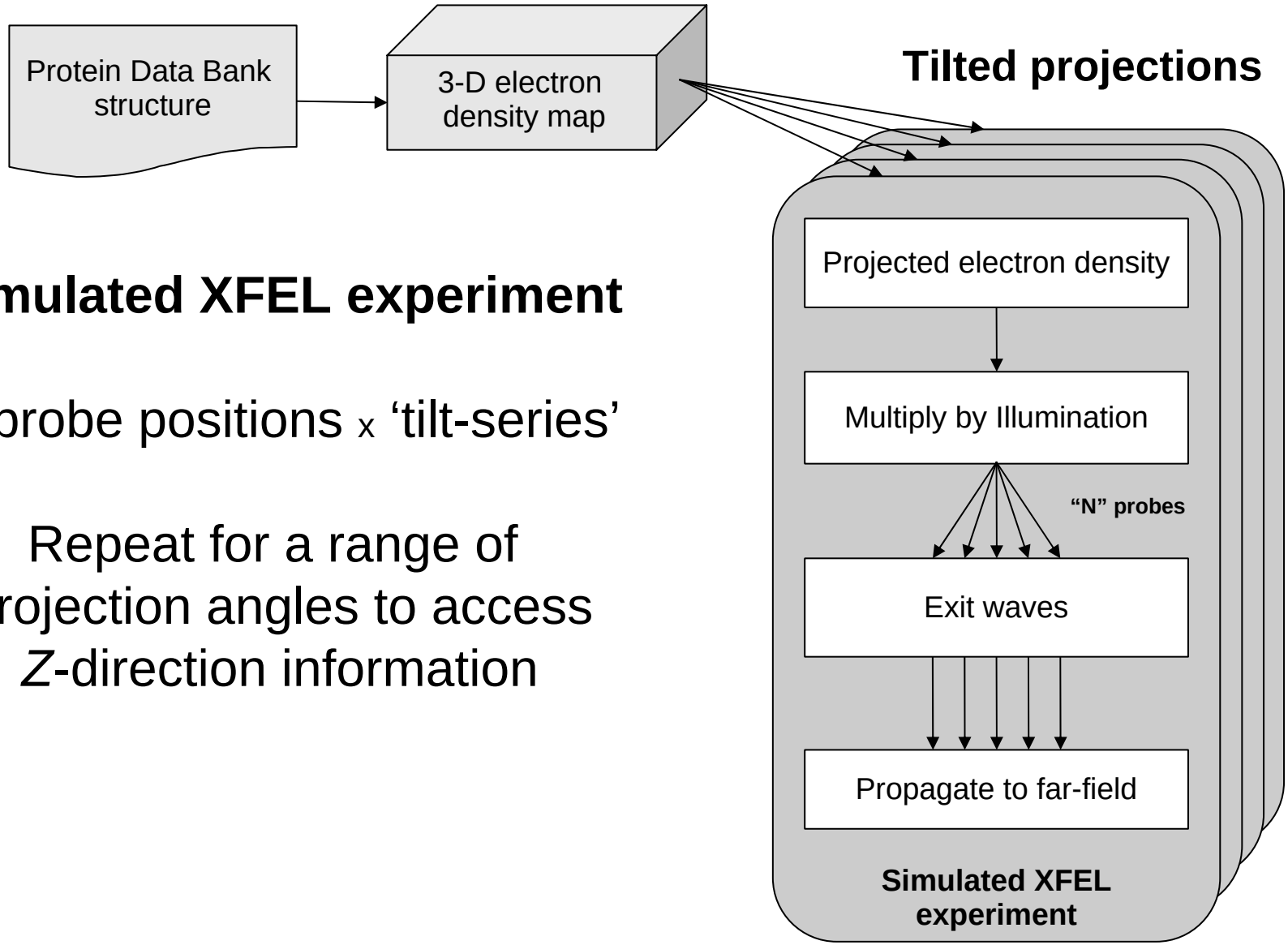

Simulated XFEL experiment

N probe positions x 'tilt-series'

Repeat for a range of projection angles to access *Z*-direction information

Simulated tilt-series

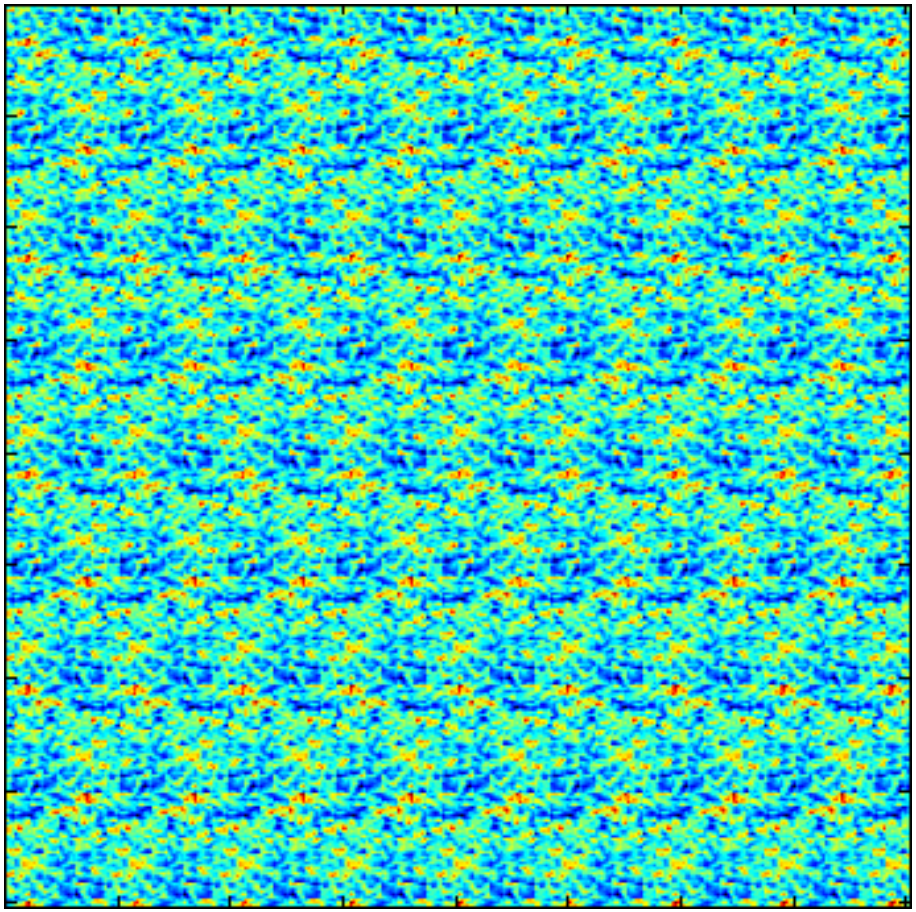

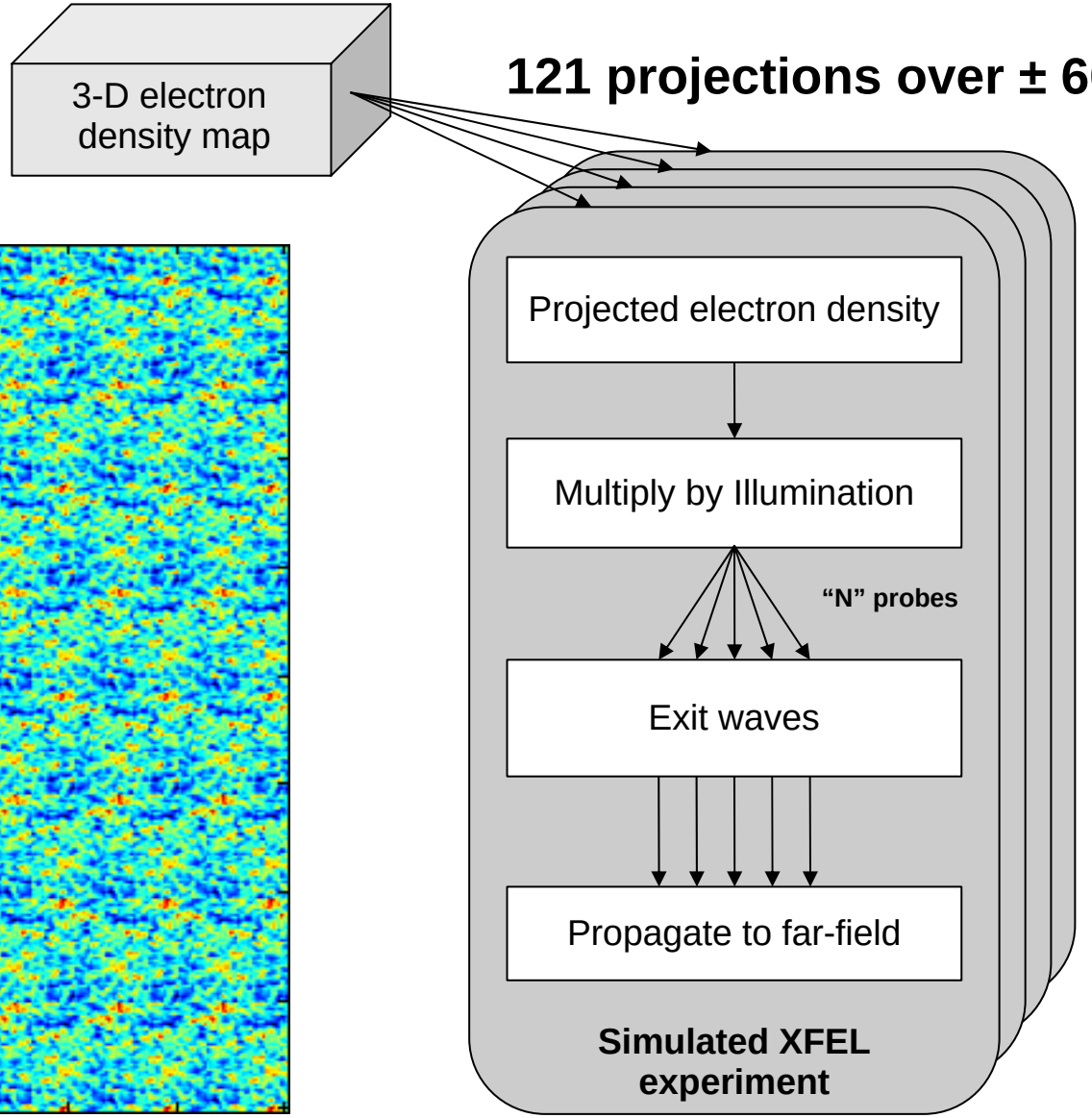

Tomographic reconstruction of protein

$$f_i^{new} = f_i^{old} + \gamma \frac{\left(p_j^{new} - p_j^{old}\right)}{\sum_{k=1}^{I} w_{kj}^2} w_{ij}$$

Handles missing Fourier coefficients using a weighting matrix, w_{ij}

Relaxation factor γ aids convergence

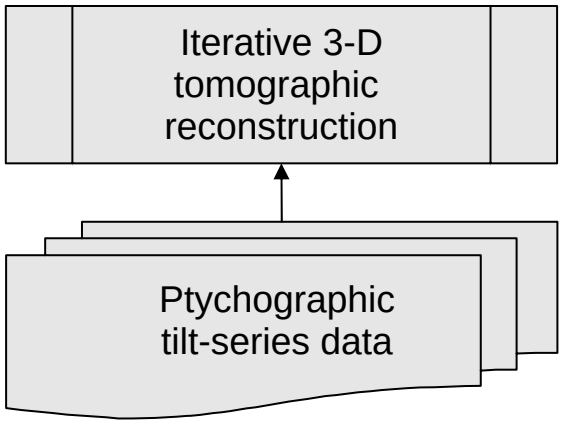

Reconstruction of 3D electron density

Algebraic Reconstruction Technique (ART):

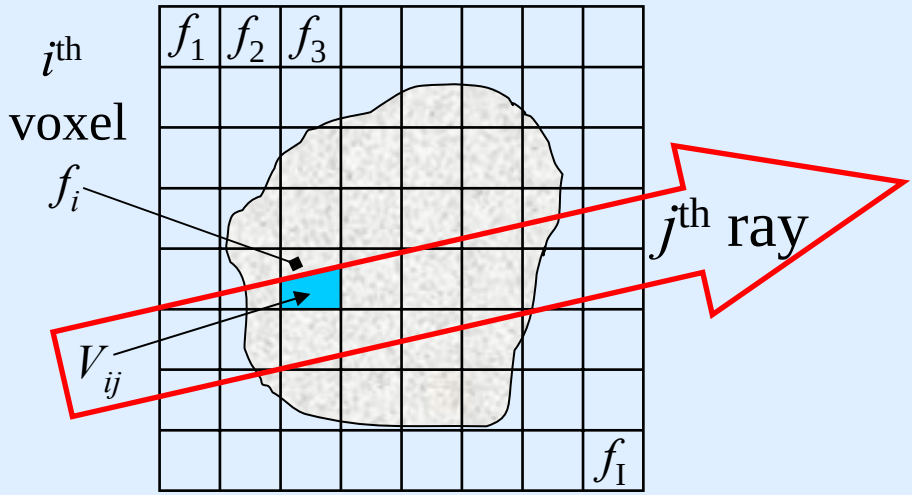

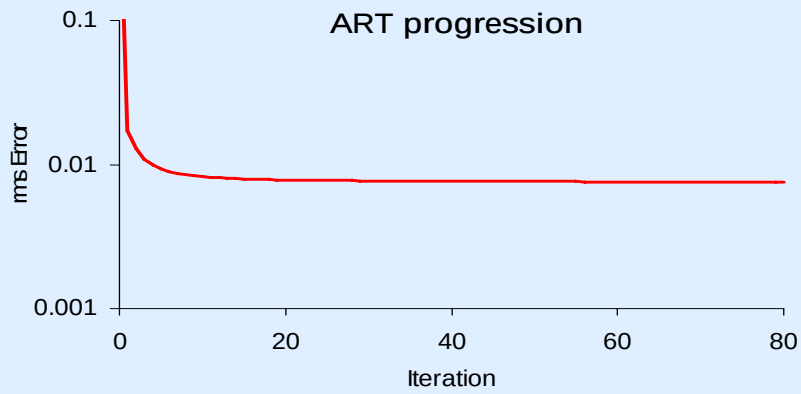

Reconstructed 3-D electron density map

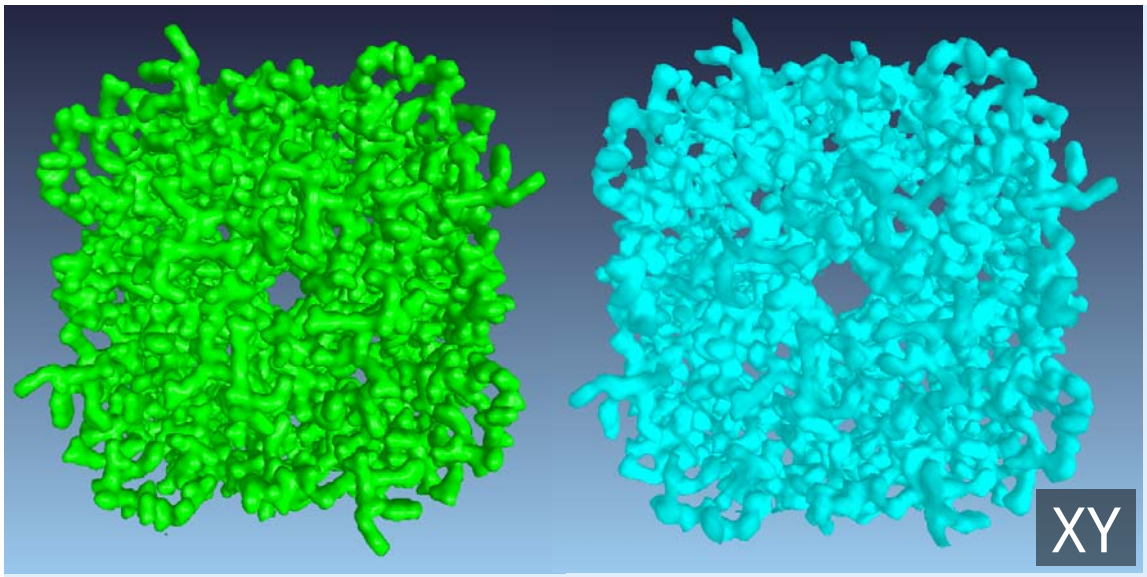

Isosurface rendered at 0.5 e/Å^2

Reconstructed projections agree well with original data

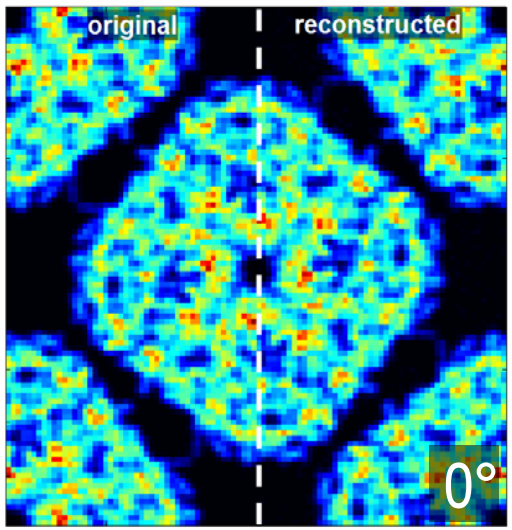

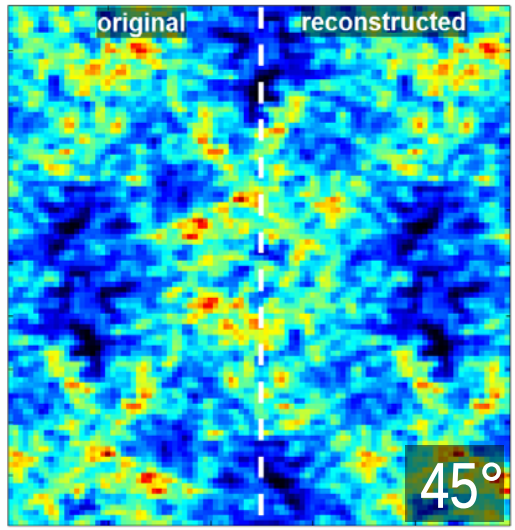

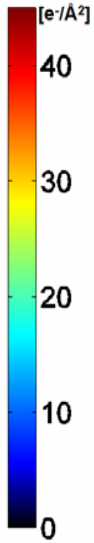

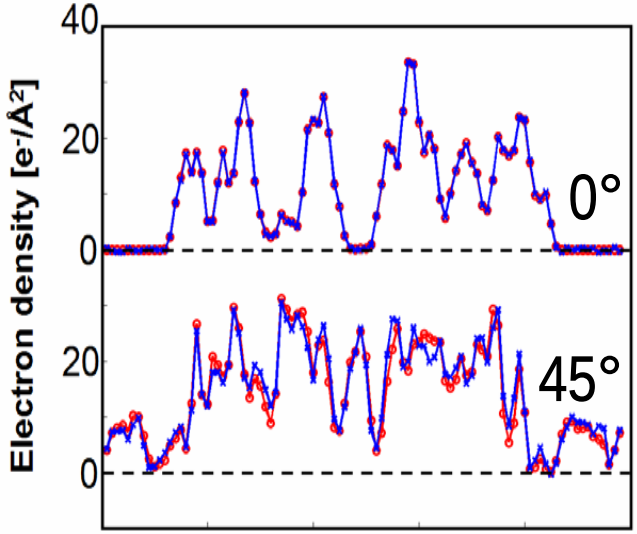

Reconstrcuted 3-D electron density map

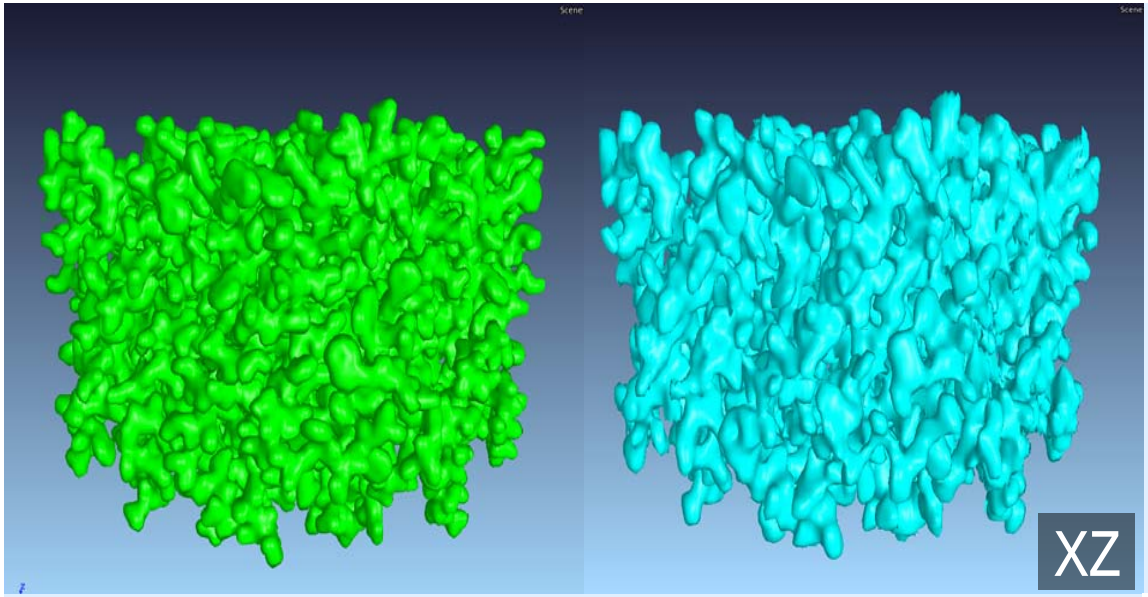

Isosurface rendered at 0.5 e/Å^2

Slices from 3-D density map agree reasonably well with original values

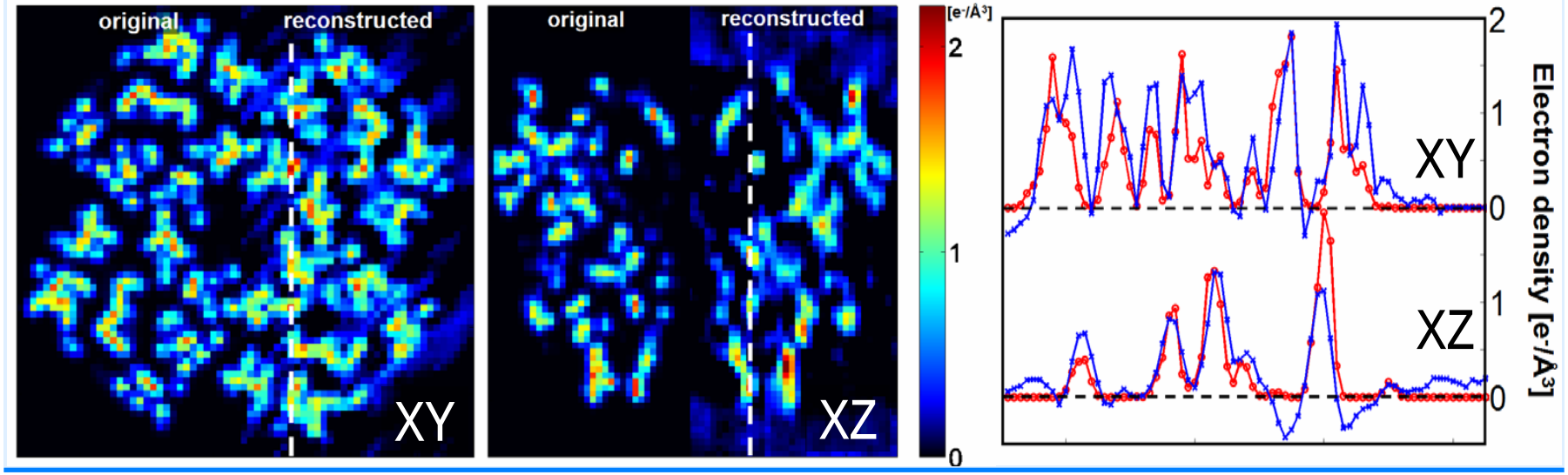

Reconstruction quality vs. Poisson noise

RMS error in reconstructed projections follows Poisson noise: As pulse intensity, or number of shots per projection is increased, the RMS error follows a log-log trend.

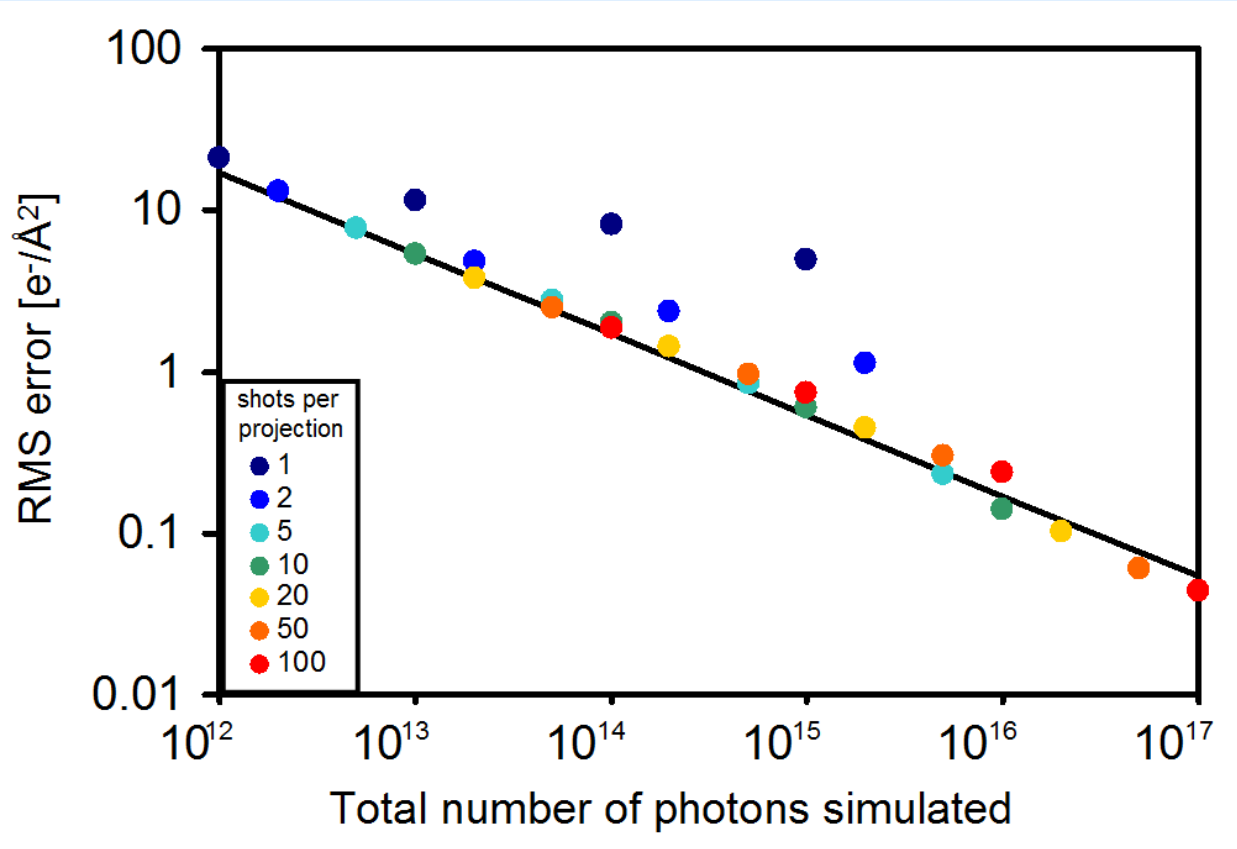

Conclusion

Thank you for your attention

Achieved:

- Finished the first ‘full cycle’ simulation: forward calculation & reconstruction
- Experiment & reconstruction seems feasible, even when including Poisson noise and expected XFEL flux values

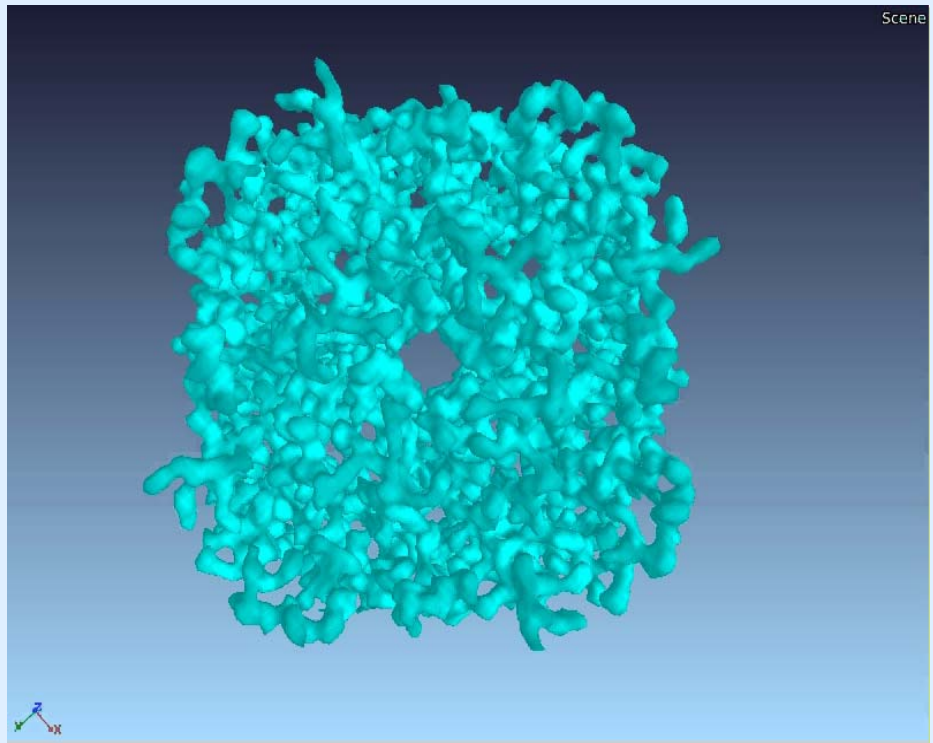

Ongoing work:

- Assess effect of variation in the incoming XFEL wave fronts
- Influence of Coulomb explosion on reconstruction
- Ewald sphere lift-off
- Experimental background …